Biogeosciences Discuss., https://doi.org/10.5194/bg-2018-360
Manuscript under review for journal Biogeosciences
Discussion started: 6 August 2018

Composition and Vertical Flux of Particulate Organic Matter to the Oxygen Minimum Zone of the Central Baltic Sea: Impact of a sporadic North Sea inflow

Carolina Cisternas-Novoa*, Frédéric A.C. Le Moigne, Anja Engel.

GEOMAR, Helmholtz Centre for Ocean Research Kiel, Düsternbrooker Weg 20, D-24105 Kiel

**Corresponding author:* Carolina Cisternas-Novoa, GEOMAR, Helmholtz Centre for Ocean Research Kiel, Düsternbrooker Weg 20, D-24105 Kiel, Germany, +49 431 600-4146 ccisternas@geomar.de

Keywords: Baltic Sea, Oxygen minimum zone, POC, PN, POP, TEP, CSP, Sediment trap, Export efficiency.

Biogeosciences Discuss., https://doi.org/10.5194/bg-2018-360
Manuscript under review for journal Biogeosciences
Discussion started: 6 August 2018

Abstract

Sinking particles are the main form to transport photosynthetically fixed carbon from the euphotic zone to the ocean interior. Oxygen (O_2) depletion may improve the efficiency of the biological carbon pump. However, how the lack of O_2 mechanistically enhances particulate organic matter (POM) fluxes is not well understood. In the Baltic Sea, the Gotland Basin (GB) and the Landsort Deep (LD) exhibit permanent bottom-water hypoxia, this is on occasions alleviated by Major Baltic Inflow (MBI), such as the one that occurred in 2014/2015 which oxygenated the bottom waters of the GB (but not of the LD). Here, we investigate the distribution and fluxes of POM in the GB and the LD in June 2015 and how they were affected by the 2015 MBI.

Fluxes and composition of sinking particles were different in the GB and the LD. In the GB, POC flux was 18% lower at 40 m than at 180 m. Particulate nitrogen (PN) and Coomassie stainable particles (CSP) fluxes decreased with depth, and particulate organic phosphorous (POP), biogenic silicate (BSi), Chl *a*, and transparent exopolymeric particles (TEP) clearly peaked within the core of the oxygen minimum zone (OMZ), which coincided with a high flux of manganese oxide (MnOx)-like particles. Contrastingly, in the LD, POC, PN, and CSP fluxes decreased 28, 42 and 56% respectively from 40 to 180m. POP, BSi and TEP fluxes, however, did not decrease with depth and only a slightly higher flux was measured at 110 m. MnOx-like particle flux was two orders of magnitude higher in the GB relative to the LD.

MnOx-like particles formed after the inflow of oxygenated water into the deep GB may form aggregates with POM. Our results suggest, that when the deep waters of GB were oxygenated (2014/2015 North Sea inflow), not only transparent exopolymeric particles, as indicated previously, but also POC, POP, BSi, and Chl *a* may bind to MnOx-like particles. POM associated with MnOx-like particles may accumulate in the redoxcline, where they formed larger particles that eventually sank to the seafloor. We propose that this mechanism would alter the vertical distribution and the flux of POM; and it may contribute to the higher transfer efficiency of POC in the GB. This is consistent with the fact that the OM reaching the seafloor was fresher and less degraded in the GB than in the LD.

Biogeosciences Discuss., https://doi.org/10.5194/bg-2018-360
Manuscript under review for journal Biogeosciences
Discussion started: 6 August 2018

1. Introduction

Understanding the downward flux of organic matter (OM) from the euphotic zone is critical to understand biogeochemical cycles in the ocean. Sinking particles are the primary vehicles for transporting photosynthetically fixed carbon from the surface to the deep ocean (Boyd and Trull, 2007; Turner, 2015). It has been suggested that the transfer of particulate organic carbon (POC) from the euphotic zone to the ocean interior is enhanced in oxygen minimum zones (OMZs) (Cavan et al., 2017; Devol and Hartnett, 2001; Engel et al., 2017; Keil et al., 2016; van Mooy et al., 2002). Possible mechanisms explaining the higher POC transfer include: i) the reduction of aggregate fragmentation due to the lower zooplankton abundance within the OMZ (Cavan et al., 2017; Keil et al., 2016); ii) a higher refractory nature of sinking particles (Keil et al., 2016; van Mooy et al., 2002); iii) a decrease in heterotrophic microbial activity due to oxygen limitation (Devol and Hartnett, 2001); and iv) the preferential degradation of nitrogen-rich organic compounds (Kalvelage et al. 2013; Van Mooy et al. 2002, Engel et al. 2017). However, mechanisms of how low O_2 concentration would affect the composition and fate of sinking OM, and the efficiency of the biologic carbon pump in oxygen deficient basins have hardly been investigated.

The semi-enclosed, brackish Baltic Sea is a unique environment with strong natural gradients of salinity and temperature (Kullenberg and Jacobsen, 1981), primary productivity, nutrients (Andersen et al., 2017), and O_2 concentrations (Carstensen et al., 2014a). New production, defined as the fraction of the autotrophic production supported by allochthones sources of nitrogen (Dugdale and Goering, 1967) is considered equivalent to the particulate OM export (Eppley and Peterson, 1979; Legendre and Gosselin, 1989) on appropriate timescales. In the Baltic Sea, new production varies seasonally (Thomas and Schneider, 1999); spring and summer are periods of elevated new production supported by the diatom-dominated spring bloom and by diazotrophic cyanobacteria, respectively (Wasmund and Uhlig, 2003). Based on sediment trap data, collected at 140 m in the Gotland Basin, Struck et al. (2004) reported that the highest fluxes of POC occur in fall, followed by summer and spring. Using $\delta^{15}N$ they showed that during the

summer, N_2 fixation by diazotrophic species was the primary source (~41%) of the exported nitrogen, and that the majority of the particulate OM sedimenting in the central Baltic Sea is of pelagic origin.

OM export from the euphotic zone to the seafloor has a dual significance in the deep basins of the Baltic Sea. On the one hand, it contributes to the long-term burial of POC, and consequently to the removal and long term storage of CO_2 from surface waters (Emeis et al., 2000; Leipe et al., 2011); on the other hand, it connects the pelagic and the benthic systems contributing to the oxygen consumption and hence deoxygenation at depth. Environmental and anthropogenic changes may alter the magnitude and composition of OM transferred from the surface to the seafloor in the Baltic Sea (Tamelander et al. 2017). On the long term, a decrease in OM downward flux may limit the oxygen depletion. However, to fully suppress hypoxia enhanced ventilation would be necessary the bottom waters of the Baltic Sea.

The Gotland Basin (GB) and the Landsort Deep (LD) are the deepest basins of the Baltic Sea. They exhibit permanent bottom-water hypoxia (Conley et al. 2002), caused by a combination of limited water exchange with the North Sea through the Kattegat Strait, strong vertical stratification, and high production /remineralization of OM due to eutrophication (Carstensen et al., 2014b; Conley et al., 2009). The Baltic Sea is naturally prone to hypoxia due to physical factors such as permanent salinity stratification and restricted water exchange with the ocean. From the1950s to 1970s, the hypoxic zones (<60 µmol O_2 kg^{-1}) in the Baltic Sea had expanded fourfold (Carstensen et al. 2014). North Sea inflows are the primary mechanism renewing deep water in the central Baltic Sea. A Major Baltic Inflow (MBI) occurred in 2014/2015 (Mohrholz et al. 2015); this event ventilated bottom waters for five months between February and July 2015 (Holtermann et al., 2017). Saltier, denser, O_2-rich North Sea waters entered the western Baltic Sea in December 2014 and reached the Gotland Basin on February 2015. This caused the intrusion of O_2 to deep hypoxic waters, a substantial temperature variability, and high turbidities that may be associated with redox reactions products (Schmale et al., 2016). At the time of sampling, this MBI also affected the neighboring Faroe Deep; but not the LD, located further northwest. At the LD,

water properties did not change due to the MBI, the sulfidic layer was maintained (hydrogen sulfide, H_2S concentrations of 20.7- 21.2 μM), and salinity varied between 10.6 and 10.9 (Holtermann et al., 2017).

In the GB and the LD, a permanent transition zone of about 15 to 20 m thickness separates the surface oxygenated and the anoxic waters. This zone is known as "pelagic redoxcline" and it is only disrupted by sporadic intrusions of saline, well-oxygenated waters from the North Sea (Günter et al., 2008). In the GB, the 2014/2015 MBI oxygenated the deep water column, removed the sulfidic waters in the deeper layers below the redoxcline, and created a secondary near-bottom redoxcline (Schmale et al., 2016). A steep redox gradient characterizes the pelagic redoxcline; here electron acceptors and their reduced counterparts are vertically segregated, and biogeochemical transformations mediated by microbial processes are actively occurring (Bonaglia et al., 2016; Brettar and Rheinheimer, 1991; Neretin et al., 2003). For instance, iron (Fe) and manganese (Mn) undergo rapidly reversible transformations at the redox interface. Under anoxic conditions, these metals are present in dissolved reduced forms Mn(II) and Fe(II); under oxic conditions they form particulate oxides, when react with O_2 or nitrate. Manganese oxides (MnOx) production may be microbially mediated (Neretin et al., 2003; Richardson et al., 1988), or authigenic (Glockzin et al., 2014). The reduction of Mn(IV) with sulfide occurs within a scale of seconds to minutes (Neretin et al., 2003), and is inhibited by nitrate (Dollhopf et al., 2000). The sporadic oxygenation of the deep water of the GB combined with the release of Mn from the sediments into the water column (Lenz et al., 2015) generate appropriate conditions for particulate MnOx formation. MnOx particles have previously been observed in pelagic redoxclines in the Baltic Sea (Glockzin et al., 2014; Neretin et al., 2003). They are amorphous or star-shaped particles that can occur as single particles or form aggregates enriched in OM (Neretin et al., 2003), specifically in transparent exopolymer particles (TEP) (Glockzin et al., 2014). TEP are highly sticky, polysaccharide-rich particles that can enhance aggregation and the formation of marine snow (Engel, 2000; Logan et al., 1995). Thus, MnOx-OM aggregates may significantly contribute to the downward flux of POC. However, TEP are less dense than seawater (Azetsu-

Scott and Passow, 2004); therefore they could also reduce the density of marine aggregates and decrease their sinking velocity if the ratio of dense particles to TEP is too small (Azetsu-Scott and Passow, 2004; Engel and Schartau, 1999; Mari et al., 2017). Mixed aggregates containing MnOx and TEP have reported before for the GB and LD (Dellwig et al. 2010; Glockzin et al. 2014). Their sizes ranged between 0.8 and 41 μm equivalent spherical diameter, and their sinking velocity (0.76 m d^{-1}) was lower than what was predicted by the Stokes' law (Glockzin et al., 2014) possibly due to their star-shaped morphology and the high OM content attached to them. Additionally, MnOx aggregates may affect the cycling of particle-reactive elements like phosphorous and trace metals via scavenging processes (Dellwig et al., 2010). To date, there are no measurements of the density of MnOx-OM aggregates, their potential ballast effect of sinking OM, or their effect on the flux of particle-reactive elements in the Baltic Sea.

In this study, first, we characterize the amount and composition of particles sinking out of the euphotic zone in two deep basins of the Baltic Sea: the GB and the LD. Second, we compare the sinking fluxes of POM at two stations with different O_2 concentrations below pycnocline (70 m): the GB affected by the MBI that changed the increased the O_2 concentration in the deep waters (between 140 and 220 m) and the LD that was not affected by the MBI and exhibited low O_2 concentration and sulfidic conditions in the deep water (from 74 to 430 m). We hypothesize that the different O_2 conditions in the water column of the GB compared with the LD, affected the formation of MnOx rich-aggregates and subsequently OM distribution causing differences in degradation and export of OM between those two stations.

2. Methods

2.1. Sampling location and water column properties

Samples were collected during the BalticOM cruise in the Baltic Sea onboard the *RV Alkor* form June 3th to June 19th, 2015. We collected sinking particles using surface-tethered sediment traps (Engel et al., 2017; Knauer et al., 1979) in the GB and the LB (Fig.1). Additionally, water column samples were collected using a Niskin-bottle rosette at the locations of the trap deployments. Temperature, salinity and O_2 concentration were determined at each station using a conductivity

temperature depth (CTD, Sea-Bird) instrument with an Oxyguard (PreSens) oxygen sensor, calibrated with discrete samples measured using the Winkler method (Strickland and Parsons, 1968; Wilhelm, 1888).

2.2. Sediment trap design and deployment

We deployed two surface-tethered sediment traps for two days in the GB, and one day in the LD (Fig.1). Each trap collected particles at four depths between 40 and 180 m (Table 1) to estimate POM fluxes to and within the OMZ. The sediment trap consisted in five arrays of 12 acrylic particle interceptor tubes (PITs) mounted in a PVC cross frame; each tube was equipped with an acrylic baffle at the top to minimize the collection of swimmers (Engel et al., 2017; Knauer et al., 1979). Two particle collector arrays were located at 40 m to estimate the replicability of the system. The PITs were 7 cm in diameter and 53 cm in height with an aspect ratio of 7.5 and a collection area of 0.0038 m^{-2}. The cross frame and PITs were attached to a line that had a bottom weight and a set of surface and subsurface floats. The procedures for PIT preparation and sample recovery followed Engel et al. (2017). Shortly before deployment, each PIT was filled with 1.5 L of seawater previously filtered through a 0.2 µm pore size cartridge. A preservative solution of saline brine (50 g L^{-1}) was added slowly to each PIT and underneath the 1.5 L of filtered seawater, carefully keeping the density gradient. The PITs were kept caped until deployment and again immediately after recovery to avoid contamination. After recovery, the density gradient was visually verified. Then, the supernatant seawater was siphoned off the PIT, the remaining bottom waters (approx. 0.6 L) containing the particles were pooled together and filled-up to 10L with filtered seawater. After that, the samples were screened with a 500 µm mesh to remove swimmers. Subsequently, samples were split into aliquots that were processed for the different biogeochemical analysis as described in Engel et al. (2017).

2.3. Biogeochemical analysis

Nutrients were measured in unfiltered seawater samples of the deployment stations. Ammonium (detection limit 0.05 µM) was measured directly on board after Solórzano (1969). Phosphate, nitrate, and nitrite (detection limit 0.04 µM) were stored frozen until their analysis; samples were

measured photometrically with continuous flow analysis on an auto-analyzer (QuAAtro; Seal Analytical) after Grasshoff et al. (1999).

Particulate organic carbon (POC), nitrogen (PN), organic phosphorous (POP), and chlorophyll a (Chl *a*) were determined as described in Engel et al. (2017). Aliquots of 100 to 200 ml of the trapped material, and 500 ml for the sampled seawater were filtered in duplicated for each parameter at low vacuum (<200 mbar), onto pre-combusted GF/F filters (8h at 500°C). After filtration, the filters were stored frozen (-20°C) until analysis. Prior analysis, filters for POC-PN determination were exposed to acid fumes (37% hydrochloric acid) to remove carbonates, and subsequently dried for 12h at 60 °C. POC and PN concentrations were determined using an elemental analyzer (Euro EA, Hechatech) after Sharp (1974).

POP was analyzed after Hansen and Koroleff (1999). POP was oxidized to orthophosphate by heating the filters in 40 mL of deionized water (18.2MΩ) with Oxisolv (MERCK 112936) for 30 min in a pressure cooker. Orthophosphate was determined spectrophotometrically at 882 nm in a Shimadzu UV-VIS Spectrophotometer UV1201.

Chl *a* was analyzed after extraction with 10 mL of 90% acetone, the fluorescence of the samples was measured using a Turner fluorimeter (Turner, 10-AU) according to Strickland et al. (1972). The fluorometer was calibrated with a standard solution of Chl *a* (Sigma-Aldrich C-5753).

Phytoplankton composition and abundance in the stations where we deployed sediment traps was characterized microscopically and using a flow cytometer. Phytoplankton, > 5 µm, was counted and identified in 50 ml of fixed samples (Lugol's solution, 1% final concentration) using a Zeiss Axiovert inverted microscope (200x magnification). The size of the counted phytoplankton species ranged from 10 to 200 µm. Phytoplankton, <20 µm, cell abundance was quantified using a flow cytometer (FACSCalibur, Becton, Dickson, Oxford, UK). 2 ml samples were fixed with formaldehyde (1% final concentration) and stored frozen (-80 °C) until analysis (two weeks later). Cell counts were determined with CellQuest software (Becton Dickenson); pico- and nanoplankton populations of naturally containing chlorophyll or phycoerythrin (*i.e.*, Synechococcus) were identified and enumerated.

Biogenic silica (BSi) was determined by filtering duplicate aliquots of 50 to 100 mL onto 0.4 µm cellulose acetate filters. Samples were stored at -20°C until analysis. For the measurements, filters were digested in NaOH at 85°C for 135 min; the pH was adjusted to 8 with HCl. Silicate was measured spectrophotometrically according to Hansen and Koroleff (2007).

Transparent exopolymeric particles (TEP) and coomassie stainable particles (CSP) from trap and water column were analyzed by microscopy according to Alldredge et al. (1993) and Long and Azam (1996) respectively. Duplicate aliquots of 5 to 20 ml were filtered onto 0.4 µm Nuclepore membrane filters (Whatmann) and stained with 1 ml of Alcian Blue solution for TEP and Coomassie brilliant blue solution for CSP. Filters were transferred onto Cytoclear ® slides and frozen (-20°C) until microscopy analysis. Thirty images for each filter were captured under 200x magnification using a light microscope (Zeiss Axio Scope A.1) connected to a color camera (AxioCam MRc). Particle number and area was measured semi-automatically using WCIF ImageJ software. Image analysis of TEP and CSP were conducted after Engel (2009). Additionally, TEP and CSP in water samples from the stations where we deployed sediment traps were analyzed spectrophotometrically according to Passow and Alldredge (1995) and Cisternas-Novoa et al. (2014) respectively.

MnOx-like particle abundance was determined microscopically using the same images that for TEP and CSP determination and a modification of the method described above. Thirty images per filter (200x) were analyzed semi-automatically using Image J. The RGB image was split in three channels: red, blue and green, and the blue, instead of the red channel, was used to quantify the amount of MnOx-like particles in the water column and sediment traps, in this manner the MnOx-like particles were clearly visible with a negligible disruption from TEP or CSP stained blue.

Total amino acids (TAA) were analyzed directly in the unfiltered seawater and trapped material. Samples were stored at -20°C until analysis. Duplicate samples were hydrolyzed at 100 °C in 6N HCl (Suprapur® Hydrochloric acid 30%) and 11 mM ascorbic acid for 20 h. Amino acids were separated and measured by high-performance liquid chromatography (HPLC), after derivatization with ortho-phthaldialdehyde using a fluorescence detector (Excitation/Emission 330/445 nm) (Dittmar et al., 2009; Lindroth and Mopper, 1979).

Total combined carbohydrates (TCHO) were determined by ion chromatography according to Engel and Händel (2011). TCHO were analyzed directly in the unfiltered seawater and sediment trap material. Samples were stored at -20°C until analysis. Prior to analysis, the samples were desalted by membrane dialysis using dialysis tubes with 1 kDa molecular weight cut-off (Spectra Por). The desalination was conducted for 4.5 h at 1°C. Then, a 2 mL subsample was sealed with 1.6 mL 1M HCl in pre-combusted glass ampoules and hydrolyzed. Samples were hydrolyzed for 20 h at 100°C. After hydrolysis, the subsamples were neutralized by acid evaporation under N_2 atmosphere at 50°C, resuspended with ultrapure Milli-Q water and analyzed by ion chromatography.

2.4 Statistics

A Mann-Whitney U-test was used to test for significant differences between two parameters. The results of statistical analyses were assumed to be significant at *p*-values < 0.05. Statistical analyses were performed using Matlab software (MatlabR2014a).

3. Results

3.1. Biogeochemistry of the water column

The water column of both stations was stratified during the study. Deeper in the water column, a pycnocline (halocline) coincided with the oxycline and was located between 63 and 80 m in the GB and between 55 and 75 m in the LD (Fig. 2). Additionally, a seasonal thermocline was located between 20 and 30 m in the GB and between 12 and 38 m in the LD. The GB had a hypoxic layer (<60 µmol O_2 L^{-1}) between 74 and 140 m and the core of the OMZ (<10 µmol O_2 L^{-1}) was located between 96 and 125 m. The increasing oxygen concentrations at depth (>140m) can be related to the MBI event in 2014/2015 that ventilated the otherwise anoxic deep layer of the GB (Holtermann et al., 2017) and caused a rise in O_2 concentration from less than 40 µmol O_2 L^{-1} at 140 m to 79 µmol O_2 L^{-1} at 220 m (Fig. 2a). The MBI, however, did not reach the LD (Fig. 2b), where oxygen was below the detection limit (<3 µmol O_2 L^{-1}) from 74 m to the bottom (430 m). The vertical profile of nutrients was different at both stations (Fig. 2). In the GB, nitrate increased from below the detection limit in the surface waters to 0.17 µM at 40 m. Nitrate concentrations

were variable within the OMZ (6 μM at 80 and 140 m, and 0.12 μM at 110 m). At 220 m nitrate concentration decreased to 4.8 μM (Fig. 2a). Nitrite was below the detection limit in most of the water column except for 60 m (0.09 μM) and 110 m (0.11 μM). Ammonium increased from 0.14 μM in the surface to 1.15 μM at 60 m; concentrations were variable in the OMZ with less than 0.15 μM at 80 and 140 m, and maximum concentration of 3.28 ± 0.01 μM at 110m. Vertical profiles of phosphate and silicate at the GB were similar; the concentrations steadily increased from the surface (0.29 μM and 10.36 μM respectively) to the OMZ (2.67 μM and 39.07 μM respectively), and gradually decreased below the OMZ (Fig. 2a). Hydrogen sulfide was not detectable in the GB.

In the LD, nitrate and nitrite concentrations were below the detection limit between the surface and 250 m (<0.06 μM) (Fig. 2b). Ammonium concentrations varied between 0.06 and 0.59 μM in the upper 70 m and increased to 5.97 and 8.03 μM in the OMZ. The lowest concentration (0.07μM) was measured in the surface and maximum concentration of 8.03 μM at 110 m. Phosphate and silicate concentrations varied between 1.58 ± 0.04 (at 40 m) and 2.18± 0.80 μM phosphate and between 21.75 ± 4.78 (at 40 m) and 35.67 ±14.59 μM silicate in the upper 110 m of the water column; lowest concentrations were measured at 180 m (0.2 2 μM and 7.4 μM respectively). Highest concentrations of nitrate and nitrite (6.01 and 0.22 μM) were observed at 400 and 350 m, respectively. Hydrogen sulfide was measurable below 180 m, with the highest concentration (3.97 μM) measured at 250 m and the lowest (0.04 μM) between 300 and 350 m (Fig. 2b).

3.2. Particulate organic matter concentration in the water column

Chl *a* concentration in the upper 10 m was slightly higher in the GB (1.5-1.7 μg L^{-1}, Fig. 3b) than in LD (1.4-1.2 μg L^{-1} and 0.1-0.3 μM, Fig. 3e). This agrees with estimates of integrated total primary production, which were 380 mg C m^{-2} d^{-1} in the GB and 334 mg C m^{-2} d^{-1} in the LD (Piontek et al., unpublished). Pico- (<2 μm) and nanophytoplankton (2-20 μm) abundances, as determined by flow cytometry, were higher in the upper 60 m, although detectable in the entire

286 water column. Pico- and nanophytoplankton abundances were 10% higher in GB than in LD
287 (Table 2). Phycoerythrin fluorescence, mainly from picophytoplankton (92% in GB and 96% in
288 LD), was 30% higher in GB than in LD.
289 The abundance of larger phytoplankton (>5 μm) was determined by microscopy. Microscopic
290 counts of cells showed about 63% higher phytoplankton abundance in the LD than in the GB
291 (Table 3). Filamentous, unicellular cyanobacteria dominated the large phytoplankton community
292 at both stations with up to 90% corresponding to *Aphanizomenon* sp. Cyanobacteria were 60%
293 less abundant in the GB than in the LD (Table 3). They represented 56% of the total
294 phytoplankton counts in the GB and up to 74% in the LD. Dinoflagellates (dominated by
295 *Dinophysis* sp.) were significant in both stations (19%), whereas chlorophytes (dominated by
296 filaments of *Planctonema* sp. containing cylindrical cells) were more abundant in the GB than in
297 LD (25% and 4% of the total respectively). Diatoms represented less than 1% of the
298 phytoplankton in both stations, and they were slightly more abundant at 40 m in the LD (Table 3).
299 BSi was higher in the upper 10 m (0.4-0.5 μM) and decreased with depth in the GB (Fig. 3b),
300 whereas in the LD, BSi showed a peak at 40 m and then decreased with depth (Fig. 3f).
301 Vertical profiles of POC, PN, and POP concentration were similar in the water column of the two
302 stations (Fig. 3a, d). In the GB, the concentrations were higher in the surface (POC: 40.38 ± 0.80,
303 PN: 3.89± 0.01, and POP: 0.26± 0.04 μM) and decreased gradually with depth until 110 m where
304 relatively high concentrations (POC 18 ± 0.63, PN: 2± 0.08, and POP: 0.2 μM) were observed.
305 The lowest concentrations were found at 180 m (POC: 11.97 ± 1.03, PN: 1.05± 0.02, and POP
306 <0.03 μM) (Fig. 3a). In the LD, POM decreased with depth from the surface (POC: 35 ± 0.99,
307 PN: 4± 0.09, and POP: 0.2 μM) to 40 m, remained relatively constant between 40 and 80 m and
308 decreased again between 110 and 250 m (Fig. 3d).
309 We observed high concentrations of TEP and CSP in the upper 10 m in both stations. The highest
310 TEP concentration was measured at 1 and 10 m at both stations, and it was slightly higher (19%)
311 in the GB than in the LD (Fig. 3c, f). TEP and CSP vertical profiles were different from each
312 other in the GB (Fig. 3c) and covaried in the LD (Fig. 3f). Like observed for POC, PN, and POP,

TEP concentrations showed a peak at 110 m (50.29± 6.17 μg XG eq. L^{-1}) in the GB. The highest concentration of CSP at this station was observed in the shallowest (1 m) sample, CSP concentration decreased quickly at 10 m, and then it increased at 140 and 230 m (the deepest sample ~20 m above the seafloor) (Fig. 3c). In the LD, the highest concentrations of TEP and CSP were measured in surface (1 and 10 m) and at 110 m (Fig. 3f). TEP and CSP decreased with depth in the first 80 m (from 53.26± 7.10 to 18.39± 4.57 μg XG eq. L^{-1} and from 53.26± 7.10 to 31.57± 18.78 μg BSA eq. L^{-1}). Both types of gel-like particles showed an increase in concentration at 110 m (49.25± 4.08 μg XG eq. L^{-1} and 66.89± 22.33 μg BSA eq. L^{-1} respectively). Bellow 110m, TEP concentrations stayed relatively constant, while CSP concentrations decreased at 180 m and kept relatively constant below that depth.

3.3. MnOx-like particles vertical distribution in the water column

Dark, star-shaped, MnOx-like particles (Glockzin et al., 2014; Neretin et al., 2003) were observed below the fully oxygenated mixed layer in the GB and, in less abundance, in the LD (Fig. 4). In GB, single MnOx-like particle and large aggregates were observed from 80 m to 220 m (the deepest sample, approximately 28 m above the seafloor). Relatively high concentration of MnOx-like particles (2×10^6 particles L^{-1}), were measured in the upper (80 m) and lower (140 m) oxycline where the O_2 concentration was less than 40 μM, and at 220 m (4×10^6 particles L^{-1})(Fig. 4a). The lowest abundance of MnOx-like particles (7×10^5 particles L^{-1}) was observed at 110 m, in the core of the OMZ where the O_2 concentration was less than10 μM. The ESD varied between 0.6 and 30.5 μm and the median was 3.0 μm. The largest aggregates were observed in the upper oxycline (80 m). In the LD, MnOx-like particles were less abundant, smaller and had a narrow distribution in the water column than in the GB. MnOx-like particles were not detected in the fully oxic (0-40 m) or fully anoxic (180 to 430 m) water column. At 60 m, right above the oxycline, MnOx-like particles began to appear, however, in relatively low abundance. The maximum abundance, 9×10^5 particles L^{-1}, was observed in the oxycline at 70 m (Fig. 4b). The ESD varied ranged between 0.6 and 13.4 μm, the largest aggregates were observed at 70 m.

3.4. Fluxes of Particulate Organic Matter

Fluxes of particulate organic matter varied little with depth in the GB (Fig. 5a-c). POC flux slightly increased by 18% from the shallowest (40 m) to the deepest (180 m) depth. Fluxes of PN and CSP were higher at 40 and 60 m and decreased by 19 and 70% from 60 to 180 m, respectively (Fig. 5a and 5c). On the other hand, fluxes of POP, BSi, Chl *a* (Fig. 5b) and TEP (Fig. 6a) peaked at 110 m. Those fluxes increased by 68, 61, 44 and 68% respectively from 40 m to 110 m; then they decreased by 22, 65, 27 and 19% from 110 m to 180 m. This increment of fluxes at 110 m coincided with the presence of abundant MnOx-like particles associated with TEP (Fig. 6a). In addition, TEP size distribution, determined by image analysis, indicated an increase in large TEP at 110 m (data not shown). In contrast, in the LD, POC, PN (Fig. 5d) and CSP (Fig. 6d) fluxes decreased with depth. Fluxes were 28, 42 and 56% less at 180 than at 40 m. However, the POP, BSi (Fig. 5e) and TEP (Fig. 6c) showed highest fluxes at 110 m.

MnOx-like particles were drastically less abundant in sediment trap samples from the LD than in the GB and when present, only as single particles not as aggregates with TEP or CSP (Fig. 6c, d). The flux of MnOx-like particles at 110 and 180 m was two orders of magnitude larger in the GB than in the LD (Table 4). At both stations, and similar to the water column, MnOx-like particles were not observed in sediment trap samples collected at 40 and 60 m. In the GB, MnOx-like particles were present in the sediment traps at 110 m and 180 m. MnOx- like were as single particles and forming aggregates with each other and other particles such as: TEP (Figure 6a, f), phytoplankton cells, or detrital material. The ESD of MnOx-like particles and aggregates ranged from 0.6 to 167 μm (median 2.8 μm) at 110 m and from 0.6 to 153 μm (median 3.3 μm) at 180 m. In the LD, only a few, single MnOx-like particles were observed at 110 and 180 m and their size ranged from 0.6 to 16.5 mm (media 1.8) at 110 m (Table 4).

TAA flux ranged from 371±12 to 501± 33 μmol $m^{-2}d^{-1}$ in the GB and from 502± 84 to 785± 54 μmol $m^{-2}d^{-1}$ in the LD (Fig. 7a). In the GB, the flux decreased with depth whereas, in the LD, the TAA flux at 40 m was lower than at 60 m and decreased with depth from 60 to 180 m (Fig. 7b). The TCHO flux varied between 303± 8 and 428± 14 μmol $m^{-2}d^{-1}$ in the GB (Fig. 7a) and between

503± 19 and 584± 8 μmol $m^{-2}d^{-1}$ in the LD (Fig. 7b). Vertical profile of TCHO flux was similar in both stations. TCHO flux increased from 40 to 110 m, where the highest TCHO flux was measured, and then TCHO flux decreased at 180 m. The TCHO flux at 180 m was 22% higher than at 40 m in the GB, and the same that at 40 m in the LD.

3.5. *Chemical composition of sinking and suspended OM*

Elemental ratios for sinking and suspended OM in the GB and the LD are shown in Table 5. The POC:PN ratio of the sinking OM increased with depth at both stations. In suspended OM, this ratio was more variable in the GB and decreased with depth in LD. The POC:PN molar ratio of suspended and sinking OM may be compared to the classical Redfield ratio for living plankton which is 106: 16: 1 for C:N:P(Redfield et al., 1963). Sinking OM was slightly above Redfield's at both stations. The POC:PN ratios of the sinking OM in both GB and LD were not significantly different. Contrastingly, in the suspended OM, POC:PN ratios were higher in the GB compared to the LD (p<0.001; Mann–Whitney U-test). In the LD the POC:PN of sinking OM was significantly lower than in suspended OM (p<0.001).

The POC:POP molar ratio of sinking OM was lower (p<0.05) in the GB than in the LD; and it was higher (p<0.01) in sinking than in suspended OM in the LD (Table 5). The POC:BSi molar ratio was lower in sinking than in suspended OM in both stations (GB: p<0.05; LD: p<0.01). In suspended OM, the POC:BSi ratio was above Redfield ratio, whereas in sinking OM it was below Redfield value (Table 5). The PN:POP molar ratio was lower in sinking OM than in suspended OM in both stations (p<0.001). In sinking OM this value was always below the Redfield ratio, while in suspended OM, it was always above the Redfield ratio.

At both stations, the fraction of sinking POC composed of AA was larger than in suspended OM. Similarly, the C contained in CHO made up a larger percentage in sinking OM than in suspended OM (Table 5).

The amino acid-based degradation index (DI, Dauwe et al., 1999) in sinking OM varied from 0.1 to 1.14 and was higher than in suspended OM (-1.25 to -0.42). The DI was higher in the GB than in the LD in sinking and suspended OM. In the sinking OM of the GB, the DI decreased with depth but in the LD was more positive at 110m than at 60 m (Table 5).

Biogeosciences Discuss., https://doi.org/10.5194/bg-2018-360
Manuscript under review for journal Biogeosciences
Discussion started: 6 August 2018

4. Discussion

In this study, we described the results of: 1) the characterization of the surface biogeochemical conditions and the amount and composition of the particles produced in the euphotic zone of two deep basins in the central Baltic Sea, *i.e*., the GB and the LD, during early summer 2015, and 2) the flux of sinking particles out of the euphotic zone as well as their variation at depth in the two basins. We assess the potential influence of increased O_2 concentration caused by the 2014/2015 MBI in the GB on the chemical composition and degradation stage of the sinking and suspended OM relative to the anoxic LD.

4.1 Characterization of biogeochemical conditions in GB and LD

Temperature, O_2, and inorganic nutrient concentrations were similar in surface at both stations. Moreover, though there were slight differences in biogeochemical conditions, such as primary production, phytoplankton composition and chemical composition of POM, in the surface water column, those were not significant. The concentration of Chl *a* (Fig. 3), the abundance of picophytoplankton, nanophytoplankton (Table 2) and primary production (PP, Piontek et al. unpublished data) were slightly higher (20, 10 and 10 % respectively) in the GB than in the LD. At both stations, phycoerythrin-containing cyanobacteria were a small fraction of the pico- and nano-phytoplankton. Pico-phytoplankton cell abundance (cell mL^{-1}) dominated the small phytoplankton (Table 2), suggesting a significant contribution to PP and Chl *a* concentration. These findings coincide with what was described previously for early summer, in the Baltic Sea that indicate that this period corresponded to a low productivity transition phase characterized by low Chl *a* concentration (≤ 2 µg L^{-1}) sustained mostly by nano- and picophytoplankton communities (Leppänen et al., 1995) which co-existed with cyanobacteria and other phytoplankton species (Kreus et al. 2015). Microscopic analysis of larger phytoplankton (>5 µm), on the other hand, showed that filamentous cyanobacteria *Aphanizomenon* sp. (up to 200 µm large) was the dominant type on this size fraction in the upper 40 m (Table 3). *Aphanizomenon* sp. and *Nodularia spumigena*, are known to form summer blooms in the Baltic Sea, where they accumulate at the sea surface of the thermally stratified water column (Bianchi et al., 2000;

Nausch et al., 2009; Wasmund, 1997). Cell abundance of total phytoplankton (>5 μm) were not significantly different (p=0.74) in the GB and the LD.

POC, PN, POP, BSi, TEP and CSP concentrations in the surface waters were also similar at both stations (Fig. 3). The concentration of TEP was higher than of CSP, both types of gel-like particles were most abundant in the euphotic zone indicating a phytoplankton origin. In the surface water column, TEP concentrations (48 and 62 μg X.G. Eq. L^{-1} in the GB and the LD, respectively) were 69 and 76% lower than the value previously reported for summer in the central Baltic Sea in June (200 μg X.G. Eq. L^{-1}) (Engel et al., 2002). Likewise, our dissolved inorganic nitrogen concentrations were below the detection limit in the surface; however phosphate concentrations were higher (0.2-0.65 μM) than the ones on the Engel et al. (2002) study. Mari and Burd (1998) reported that TEP concentration peaked during the spring bloom and in summer in the Kattegat. TEP production may be enhance by enviromental conditions such as nutrient limitation (Mari et al., 2005; Passow, 2002), which are characteristic of late summer in the Baltic Sea (Mari and Burd 1998). Our samples were collected right after the peak of the spring bloom (Le Moigne et al., 2017), thus, likely TEP concentrations had not reached the usually higher summer value yet since phosphate remained present in the water column (potentially not limiting the PP).Anoter possible explanation for the rather low concentrations of TEP could be that TEP may be removed from the surface by aggregation and subsequent sedimentation during the spring bloom due to the high abundance of cells and detrital particles during this time (Engel et al., 2002).

Although the composition and amount of OM in the surface waters at the two trap stations were similar, below the euphotic zone (40 m) the vertical profile of nutrients and POM concentrations were clearly different; likely due to the 2014/2015 MBI (Holtermann et al., 2017) that reached the deep waters of the GB. The MBI changed the vertical distribution and increse the concentration of O_2 in the GB compared with the LD. In the GB the oxygen-deficient zone (O_2 <40 μmol L^{-1}) was constrained between 74 and 140 m and the core of the OMZ (O_2 <10 μmol L^{-1}) between 96 and

125 m; below 140 m O_2 concentrations increased <40 µmol L^{-1}. In contrast, the LD maintained permanent suboxic (<5 µmol L^{-1}) waters below 74 m and hydrogen sulfide was detectable at 180 and 250 m (Fig. 2). In the GB nitrate concentration increased possibly as a consequence of the oxidation of reduced nitrogen compounds (e.g., ammonium, ammonia and organic nitrogen compound like urea) (Le Moigne et al., 2017) that accumulated during the stagnation (anoxic) period previous to the MBI (Hannig et al., 2007). MBIs can have a major impact on nutrient recycling. For instance, phosphorous could bind to iron hydroxides and MnOx and settle down during oxic conditions, building up a phosphate pool in the sediments that later on when the O_2 decreases close to the sediments, it may become a source of phosphate (Gustafsson and Stigebrandt, 2007) . In addition to changes in O_2 concentration, the MBI altered the redox conditions in the GB creating a secondary redoxcline at 140 m, where the O_2 and the MnOx-like particles concentration increased (Fig. 4a). One consequence of those changes is the vertical extension of the layer in which MnOx aggregates could form. A previous study showed that MnOx might precipitate from the water column of the GB following a MBI event (Lenz et al., 2015). Scavenging of phosphate into Mn or Fe oxides had been shown in previous studies (Neretin et al., 2003). Moreover, there is a downward flux of phosphate associated to particule iron and MnOx in the oxic water column to the anoxic basin where particles dissolved and phosphate is release (Gustafsson and Stigebrandt, 2007). This process may be responsible for the decrease of phosphate concentration below 110 m in our study (Fig. 2a). In contrast, in the LD, the water column remained suboxic down the sea floor (430 m), below the oxycline an increase of ammonium was observed (Fig.2) which could be an indicator for anaerobic respiration of OM, e.g., denitrification (Bonaglia et al., 2016; Hietanen et al., 2012). Low phosphate and silicate concentrations within the mixed layer due to phytoplankton consumption gradually increased below the pycnocline and decreased between 110 and 180 m.

In summary, although the GB and the LD had similar surface conditions in terms of phytoplankton production and POM stocks, during this study, we found differences the vertical concentration of POM (Fig. 3)in the GB, ventilated by the MBI, relative to the LD, a station that

remains suboxic.Our results suggest that differences in the vertical profile of O_2 may modify the redox conditions of the water column, enhancing the formation of MnOx-like particles(Fig. 4) that may aggregate with POM in the GB and changed its vertical distribution.

4.2 Potential influence of O_2 concentration and redox conditions on sinking fluxes of POM in the GB and the LD

During this study, we also investigated the effect of different O_2 concentrations and redox conditions on the fluxes of particles. Our measurement of carbon flux below the euphotic zone (40 m) were 11.7±0.82 mmol C m^{-2} d^{-1} in the GB and 19.8±1.22 mmol C m^{-2} d^{-1} in the LD. Extrapolating those measurements to annual flux we obtain 4.37±0.31 mol C m^{-2} a^{-1} in the GB and 7.44±0.46 mol C m^{-2} a^{-1} in the LD. Our results from the LD are compable with the long-term annual estimations from models that varied between 3.8 to 4.2 mol C m^{-2} d^{-1} (Kreus and Schartau, 2015; Sandberg et al., 2000; Stigebrandt, 1991) for the Baltic Sea; however, the estimations based on our results from the GB are higher than the C fluxes predicted by those models.

The vertical flux of POM was different the two studied stations; likely due to differences in O_2 concentrations that may affect POM remineralization and transport; in the GB, the POC flux between 40 and 180 m showed a small increase while PN slightly decreased from the bellow the oxycline (60 m) to 180 m. In the LD, the POC flux decreased greatly between 40 and 60 m, and remained relatively constant between 60 and 180 m; PN flux, however, decreased with depth. In the GB, and to a lower degree in the LD, we observed a distinctive peak of POP, BSi, Chl *a* and TEP fluxes at 110 m. This high flux of POM coincided with the appearance of dark, star-shaped particles (Fig. 6a, f) which may correspond to MnOx particles enriched in OM that have been described in the GB and the LD before (Neretin et al., 2003; Pohl et al., 2004). We observed a higher concentration of MnOx-like aggregates associated with TEP at 110 m in the GB. The 110 m sediment trap was located between the upper (80 m) and lower (140 m) oxycline where the MnOx-like particles are likely formed. This corresponds to the depth range where lowest O_2 concentration was measured but hydrogen sulfide (H_2S) was absent in the water column, which

allows the presence of those aggregates also at 180 m. On the contrary, in the LD, we measured H_2S at 180 m, this could explain why although those aggregates were present in this station below the oxycline (*i.e.*, 70 m) at 110 m, they dissolved in sulfidic waters, thus were not as abundant, and did not form aggregates with TEP (Fig.6c).

The presence of MnOx-containing aggregates enriched in OM (see TEP fluxes, Fig 6c) may have implications for the vertical flux of C and N in a stratified system with a pelagic redoxcline like the Baltic Sea. Under steady state, the upward diffusion and oxidation rate of the dissolved Mn are balanced by the sinking and dissolution rate of MnOx. During the Mn-oxidation, the POM could aggregate with the MnOx including particulate elements, and trace metals. Then, in the sulfidic waters, slow-sinking MnOx enriched in OM will be dissolved liberating the OM and altering the vertical distribution and the flux of all associated particle elements (Glockzin et al., 2014). The precipitation of MnOx could be enhanced by the oxygenation of the otherwise anoxic deep of the Baltic Sea caused by the 2014/105 MBI (Dellwig et al., 2018), those particles could bind with phosphorous and trace metals trapping them in the redoxcline (Dellwig et al., 2010). For example, in the Cariaco Basin, total particulate phosphorous reached their maximum flux in sediment traps close to the redoxcline (Benitez-Nelson et al., 2004; Benitez-Nelson et al., 2007). MnOx formation and scavenging of trace metal may be a relevant mechanism for transfer trace metals from the oxygenated to the anoxic deep waters (Dellwig et al., 2010). Moreover, even in the anoxic zone, the abundant aggregate associated bacteria (Grossart et al., 2006) could partially or completely degrade the organic compounds in those particles using NO_3^- or Mn^{2+} as an electron acceptor. This may be the reason why we observed a clear peak in the flux of POP, BSi, Chl a (Fig. 3a, b), TEP (Fig. 6a) and TCHO (Fig. 7a) at 110 m followed by a small decrease at 180 m in the GB. In the LD a smaller increment in the flux of POP, BSi (Fig. 3d), TEP (Fig. 6c) and TCHO (Fig. 7b) was also observed. The vertical fluxes of those compounds coincided with the abundance of MnOx particles; we assume that the MnOx aggregated not only with TEP as described before (Glockzin et al. 2014) and observed in this study (Fig. 6a) but also with POP, BSi, Chl *a*, and TCHO. On the other hand, nitrogen-rich compounds like PN (Fig. 3a), TAA (Fig.

7a), and CSP (Fig. 6a) gradually decreased with depth in the GB, suggesting that those compounds were less scavenge by MnOx organic-rich aggregates.

Primary production (PP) in the GB was 10% higher than in LD during our study (Piontek et al. unpublished data). However, the POC flux below the euphotic zone (at 40 m) was 42% higher in LD than in GB and comparable at both stations at 180 m. The fraction of PP exported as POC is termed export production (*e-ratio*) (Buesseler et al., 1992) , and it is calculated as the POC flux bellow the euphotic zone divided by the primary production. The *e-ratio* was calculated here using the ^{14}C based PP (Piontek et al. unpublished data) and carbon flux at 40 m (shallowest sediment trap depth, considered at the base of the euphotic zone). The *e-ratio* was 0.41 in the GB and 0.77 in the LD*; i.e.*, in GB 41% of the primary production was exported as POC below the euphotic zone (40 m) versus 77% in the LD). This suggests that a higher proportion of the primary production was remineralized in the euphotic zone of the GB compared with the LD. On the other hand, the transfer efficiency of POC to the deeper water column (*i.e.* the ratio of POC flux at180 m over POC flux at 40 m) was higher in the GB (115%) than in the LD (69%). The transfer efficiency of POM is largely controlled by the remineralization rate and the sinking velocity of particles (De La Rocha and Passow, 2007; McDonnell et al., 2015; Trull et al., 2008). The higher POC transfer efficiency in the GB than in the LD can be attributable to differences in the sinking velocities of the particles in those two stations. The presence of MnOx-OM rich aggregates in the GB may fast sinking organic particles that spend less time in the water column limiting the opportunity of particle- attached microbes to remineralized them. Assuming that MnOx had a density between 1.5 and 2.0 g cm^{-3} (Glockzin et al., 2014). The largest particles measured in GB (167 µm, Table 4) will have a sinking velocity based in Stokes' law between 508 and 1014 m d^{-1}. If we considered a mix aggregate that is 50% TEP, density 0.9 g cm^{-3} (Azetsu-Scott and Passow, 2004) and 50% MnOx (density 1.5 g cm^{-3}), its density would be 1.2 g cm^{-3} , and its theoretical sinking velocity will be 204 m d^{-1}. This indicate that theoretically, the largest mix aggregates composed of MnOx and TEP observed in the GB could reach 180 m (the location of our deepest sediment trap) in less than one day. However, the average measured sinking

554 velocity of MnOx in the laboratory for particles between 2 and 20 μm was 0.76 m d^{-1}, this is
555 significantly lower that the theoretical value (Glockzin et al., 2014). Glockzin et al. (2014)
556 suggested that the star shape and the content of OM were responsible for the lower than predicted
557 sinking velocity. There is not information about the amount of OM relatively to MnOx particles in
558 those mix aggregates, or how the MnOx to OM ratio may affect the density and sinking velocity
559 of larger aggregates like the ones we observed. Due to the shape and size of MnOx-OM
560 aggregates observed in our study (Fig. 6e), we could assume those are the same type of aggregates
561 described before by Glockzin et al. (2014). Although, we did not measure the sinking velocity of
562 those aggregates, we did observe a higher abundance of them associated with TEP at 110 and 180
563 m in the GB than in the LD. The formation of these organic matter rich MnOx aggregates could
564 represent an additional mechanism (see introduction) to explain why the efficiency of the OM
565 export is different under anoxic that under oxic conditions in the Baltic Sea. The oxygenation of
566 anoxic deep water in the GB caused by the 2014/2015 MBI, may have led to an enhanced
567 precipitation of manganese, iron and phosphorous particles (Dellwig et al., 2010; Dellwig et al.,
568 2018). For example, the formation of P-rich, metal oxides precipitates occur in the anoxic waters
569 of the Black Sea (Shaffer, 1986) and Cariaco Basin (Benitez-Nelson et al., 2004; Benitez-Nelson
570 et al., 2007) were higher concentration of particulate inorganic and organic phosphorous have
571 been observed in sediment traps close to the redoxcline.

572 *4.3 Differences on composition and lability of sinking and suspended organic matter in the GB*
573 *and the LD*

574 In the sections above, we discussed how similar biogeochemical conditions and the size of the
575 surface POM pool in both the GB and the LD were. We then looked at how the sinking flux of
576 OM was affected by the different O_2 concentrations in the water column. We now focus on the
577 influence of O_2 in the chemical composition of sinking and suspended POM. Suspended or slow
578 sinking POM, that spend more time in the water column, should theoretically, show a larger
579 degree of degradation (Goutx et al., 2007). Relative to the Redfield molar ratio: 106 POC:16
580 PN:POP, OM showed an enrichment in carbon, especially in sinking particles from the LD and

suspended OM from the GB (Table 5). Our measured values of POC:PN (~10) and POC:POP (between 89 and 506) in suspended OM coincide with the simulated ratio reported by Kreus et al. (2015) immediately after the culmination of the spring bloom, those relatively high ratios are consequence of the nitrogen depletion and are characteristic during the summer in the Baltic Sea. The same study had suggested that POC:POP higher than Redfield ratio might lead to an enhancement of particle export (Kreus et al., 2015), however, no direct observations had confirmed this hypothesis. Our measurements showed that the relative higher POC:POP ratios in sinking OM from LD, compared with the GB, do not lead to a higher transfer efficiency at this station. Compared to the suspended OM in the LD, the POP content was lower in the GB, possible related to scavenging of POP into MnOx aggregates (see section 3.4).

The AA based degradation index, DI (Dauwe et al. 1999) covers a wide range of alteration stages; the more negative the DI, the more degraded the samples, positive DI indicates fresh organic matter. In our study, the sediment trap material had a DI between 0.10 and 1.14, while suspended OM has a DI between -0.26 and -1.25 (Table 4). These values coincide with what reported earlier by Dauwe et al. (1999), and indicate that: first, the sinking particles collected in the sediment traps were less altered (they have a more positive DI) than the suspended OM collected in the CTD. Second, sinking particles from the GB were fresher than the ones from the LD, and the degradation stage increased with depth in both stations. The higher contribution of AA and CHO to the POC pool in sinking than in suspended OM and the AA- DI indicates that suspended OM was more degraded than sinking OM. The highest degree of degradation in suspended OM and sinking OM from the LD may be the result of a long time that light suspended OM or slow sinking particles spend exposed to degradation in fully oxygenated surface waters than dense, fast sinking particles collected in sediment traps.

The higher abundance of aggregates, formed by a combination of MnOx-like particles and OM, observed at 110 and 180 m in the GB could act as bacteria hot spots that combined with a higher O_2 concentration in the GB may increase the microbial degradation on sinking particles collected in the GB. However, the AA-DI, indicated that sinking OM was less altered and therefore more

labile than the sinking OM in the LD. This implied that in addition to the higher transfer efficiency of POC in the GB (see discussion above); the OM reaching the seafloor was fresher and less degraded. This support the idea that mix aggregates composed by MnOx and OM may be larger and faster sinking than the previously described by Glockzin et al. (2014). This explanation is mostly speculative, and based on the observation of large mixed aggregates in the 110 and 180 m traps (Fig. 6, Table 4). However, as mention in the previous section, further work on directly determines sinking velocity is required to prove this hypothesis.

Conclusion

Fluxes and composition of sinking particles were different in two deep basins in the Baltic Sea: the GB and the LD during early summer 2015. The two stations had similar surface characteristics and POM stock; however, at depth, the vertical profile of the O_2 concentration was different. The 2014/2015 MBI supplied oxygen-rich waters to the GB modifying the O_2 vertical profile and the redox conditions in the otherwise permanent suboxic deep waters. This event did not affect the LD allowing the comparing POM fluxes and composition under two different O_2 concentrations with similar surface water conditions. Export efficiency (*e-ratio*) derived from *in-situ* PP measurements and POC flux derivate from sediment traps indicated higher export efficiency in LD than in GB. However, the transfer efficiency (POC flux at 180 m over POC flux at 40 m) suggested that under anoxic conditions found in the LD, a smaller portion of the POC exported below the euphotic zone was transferred to 180 m than under re-oxygenated conditions present in the GB. Our results suggest that a new possible mechanism to explain the differences in the OM fluxes under different O_2 concentration could be the formation and prevalence of aggregates composed of MnOx and organic matter in the GB. Those aggregates were significantly larger and more abundant in the GB compared to the LD where sulfidic waters constrained their presence. We propose that after a MBI in the GB, the aggregates containing MnOx-like particles and organic matter could reached the sediments relatively fast and unaltered, scavenging not only phosphorous, as described previously (Dellwig et al., 2010), but also other organic compounds. The remineralization of this organic matter reaching the sediments may contribute to the quick re-

establishment of anoxic conditions in the sediment-water interface in the GB. The relevance of this process need to be further investigate in order to be included in O_2 budget and long-term predictions of the MBI impact in the O_2 and OM cycles.

Author Contributions

C.C.N. performed deployments, analyzed samples and wrote the manuscript. F.A.C.L.M, performed deployments and contributed to the writing of the manuscript. A.E designed and conducted the scientific program at sea and discussed and commented on the manuscript.

Acknowledgements

This research was supported by the DFG Collaborative Research Center 754 "Climate-Biogeochemistry Interactions in the Tropical Ocean" (to A.E., C.C.N. and F.A.C.L.M), by a Fellowship of the Excellence Cluster 'The Future Ocean' (CP1403 to F.A.C.L.M.), and by a DAAD short term grant (57130097 to C.C.N.). We thank Jon Roa, Tania Klüver, Scarlett Sett, Angela Stippkugel, Carola Wagner, Clarissa Karthäuser, Moritz Ehrlich, Sonja Endres, Hannes Wagner, Ruth Flerus, Sven Sturm and Christian Begler for support during traps preparation and deployments, help with experiment or analyzed samples. We Thank Judith Piontek for her contribution to the design of the scientific program at sea, Jaime Soto- Neira for useful discussion and help with figure preparation and Cindy Lee for helpful advices.

References

Alldredge, A. L., Passow, U., and Logan, B. E.: The abundance and significance of a class of large, transparent organic particles in the ocean, Deep Sea Research Part I: Oceanographic Research Papers, 40, 1131-1140, 1993.
Andersen, J. H., Carstensen, J., Conley, D. J., Dromph, K., Fleming-Lehtinen, V., Gustafsson, B. G., Josefson, A. B., Norkko, A., Villnäs, A., and Murray, C.: Long-term temporal and spatial trends in eutrophication status of the Baltic Sea, Biological Reviews, 92, 135-149, 2017.
Azetsu-Scott, K. and Passow, U.: Ascending marine particles: Significance of transparent exopolymer particles (TEP) in the upper ocean, Limnology and Oceanography, 49, 741-748, 2004.
Benitez-Nelson, C. R., O'Neill, L., Kolowith, L. C., Pellechia, P., and Thunel, l. R.: Phosphonates and particulate organic phosphorus cycling in an anoxic marine basin, Limnology and Oceanography, 49, 1593-1604, 2004.
Benitez-Nelson, C. R., O'Neill Madden, L. P., Styles, R. M., Thunell, R. C., and Astor, Y.: Inorganic and organic sinking particulate phosphorus fluxes across the oxic/anoxic water column of Cariaco Basin, Venezuela, Marine Chemistry, 105, 90-100, 2007.
Bianchi, T. S., Engelhaupt, E., Westman, P., Andrén, T., Rolff, C., and Elmgren, R.: Cyanobacterial blooms in the Baltic Sea: Natural or human-induced?, Limnology and Oceanography, 45, 716-726, 2000.
Bonaglia, S., Klawonn, I., Brabandere, L. D., Deutsch, B., Thamdrup, B., and Brüchert, V.: Denitrification and DNRA at the Baltic Sea oxic–anoxic interface: Substrate spectrum and kinetics, Limnology and Oceanography, 61, 1900-1915, 2016.
Boyd, P. W. and Trull, T. W.: Understanding the export of biogenic particles in oceanic waters: Is there consensus?, Progress in Oceanography, 72, 276-312, 2007.
Brettar, I. and Rheinheimer, G.: Denitrification in the Central Baltic: evidence for H ₂ S-oxidation as motor of denitrification at the oxic-anoxic interface, Marine Ecology Progress Series, 77, 157-169, 1991.
Buesseler, K. O., Bacon, M. P., Kirk Cochran, J., and Livingston, H. D.: Carbon and nitrogen export during the JGOFS North Atlantic Bloom experiment estimated from 234Th: 238U disequilibria, Deep Sea Research Part A. Oceanographic Research Papers, 39, 1115-1137, 1992.
Carstensen, J., Andersen, J. H., Gustafsson, B. G., and Conley, D. J.: Deoxygenation of the Baltic Sea during the last century, Proceedings of the National Academy of Sciences, 111, 5628-5633, 2014a.
Carstensen, J., Conley, D. J., Bonsdorff, E., Gustafsson, B. G., Hietanen, S., Janas, U., Jilbert, T., Maximov, A., Norkko, A., Norkko, J., Reed, D. C., Slomp, C. P., Timmermann, K., and Voss, M.: Hypoxia in the Baltic Sea: Biogeochemical Cycles, Benthic Fauna, and Management, AMBIO, 43, 26-36, 2014b.
Cavan, E. L., Trimmer, M., Shelley, F., and Sanders, R.: Remineralization of particulate organic carbon in an ocean oxygen minimum zone, Nature Communications, 8, 14847, 2017.
Cisternas-Novoa, C., Lee, C., and Engel, A.: A semi-quantitative spectrophotometric, dye-binding assay for determination of Coomassie Blue stainable particles, Limnology and Oceanography: Methods, 12, 604-616, 2014.
Conley, D. J., Björck, S., Bonsdorff, E., Carstensen, J., Destouni, G., Gustafsson, B. G., Hietanen, S., Kortekaas, M., Kuosa, H., Markus Meier, H. E., Müller-Karulis, B., Nordberg, K., Norkko, A., Nürnberg, G., Pitkänen, H., Rabalais, N. N., Rosenberg, R., Savchuk, O. P., Slomp, C. P., Voss, M., Wulff, F., and Zillén, L.: Hypoxia-Related Processes in the Baltic Sea, Environmental Science & Technology, 43, 3412-3420, 2009.
Dauwe, B., Middelburg, J. J., Herman, P. M. J., and Heip, C. H. R.: Linking diagenetic alteration of amino acids and bulk organic matter reactivity, Limnology and Oceanography, 44, 1809-1814, 1999.
De La Rocha, C. L. and Passow, U.: Factors influencing the sinking of POC and the efficiency of the biological carbon pump, Deep Sea Research Part II: Topical Studies in Oceanography, 54, 639-658, 2007.

Dellwig, O., Leipe, T., März, C., Glockzin, M., Pollehne, F., Schnetger, B., Yakushev, E. V., Böttcher, M. E., and Brumsack, H.-J.: A new particulate Mn–Fe–P-shuttle at the redoxcline of anoxic basins, Geochimica et Cosmochimica Acta, 74, 7100-7115, 2010.
Dellwig, O., Schnetger, B., Meyer, D., Pollehne, F., Häusler, K., and Arz, H. W.: Impact of the Major Baltic Inflow in 2014 on Manganese Cycling in the Gotland Deep (Baltic Sea), Frontiers in Marine Science, 5, 2018.
Devol, A. H. and Hartnett, H. E.: Role of the oxygen-deficient zone in transfer of organic carbon to the deep ocean, Limnology and Oceanography, 46, 1684-1690, 2001.
Dittmar, T., Cherrier, J., and Ludwichowski, K. U.: The analysis of amino acids in seawater. In: Practical guidelines for the analysis of seawater Wurl, O. and Raton, B. (Eds.), CRC Press, 2009.
Dollhopf, M. E., Nealson, K. H., Simon, D. M., and Luther, G. W.: Kinetics of Fe(III) and Mn(IV) reduction by the Black Sea strain of Shewanella putrefaciens using in situ solid state voltammetric Au/Hg electrodes, Marine Chemistry, 70, 171-180, 2000.
Dugdale, R. C. and Goering, J. J.: Uptake Of New And Regenerated Forms Of Nitrogen In Primary Productivity, Limnology and Oceanography, 12, 196-206, 1967.
Emeis, K. C., Struck, U., Leipe, T., Pollehne, F., Kunzendorf, H., and Christiansen, C.: Changes in the C, N, P burial rates in some Baltic Sea sediments over the last 150 years—relevance to P regeneration rates and the phosphorus cycle, Marine Geology, 167, 43-59, 2000.
Engel, A.: Determination of Marine Gel Particles. In: Practical Guidelines for the Analysis of Seawater, Wurl, O. (Ed.), CRC Press, Boca Raton 2009.
Engel, A.: The role of transparent exopolymer particles (TEP) in the increase in apparent particle stickiness (α) during the decline of a diatom bloom, Journal of Plankton Research, 22, 485-497, 2000.
Engel, A., Meyerhöfer, M., and von Bröckel, K.: Chemical and Biological Composition of Suspended Particles and Aggregates in the Baltic Sea in Summer (1999), Estuarine, Coastal and Shelf Science, 55, 729-741, 2002.
Engel, A. and Schartau, M.: Influence of transparent exopolymer particles (TEP) on sinking velocity of Nitzschia closterium aggregates, Marine Ecology Progress Series, 182, 69-76, 1999.
Engel, A., Wagner, H., Le Moigne, F. A. C., and Wilson, S. T.: Particle export fluxes to the oxygen minimum zone of the eastern tropical North Atlantic, Biogeosciences, 14, 1825-1838, 2017.
Eppley, R. W. and Peterson, B. J.: Particulate organic matter flux and planktonic new production in the deep ocean, Nature, 282, 677, 1979.
Glockzin, M., Pollehne, F., and Dellwig, O.: Stationary sinking velocity of authigenic manganese oxides at pelagic redoxclines, Marine Chemistry, 160, 67-74, 2014.
Goutx, M., Wakeham, S. G., Lee, C., Duflo, s. M., Guigue, C., Liu, Z., Moriceau, B., Sempére, R., Tedetti, M., and Xue, J.: Composition and degradation of marine particles with different settling velocities in the northwestern Mediterranean Sea, Limnology and Oceanography, 52, 1645-1664, 2007.
Grossart, H. P., KiÃ⍰Â¸rboe, T., Tang, K. W., Allgaier, M., Yam, E. M., and Ploug, H.: Interactions between marine snow and heterotrophic bacteria: aggregate formation and microbial dynamics, Aquatic Microbial Ecology, 42, 19-26, 2006.
Günter, J., Zubkov, M. V., Yakushev, E., Labrenz, M., and JÜrgens, K.: High abundance and dark CO2 fixation of chemolithoautotrophic prokaryotes in anoxic waters of the Baltic Sea, Limnology and Oceanography, 53, 14-22, 2008.
Gustafsson, B. G. and Stigebrandt, A.: Dynamics of nutrients and oxygen/hydrogen sulfide in the Baltic Sea deep water, Journal of Geophysical Research: Biogeosciences, 112, 2007.
Hannig, M., Lavik, G., Kuypers, M. M. M., Woebken, D., Martens-Habbena, W., and JÜrgens, K.: Shift from denitrification to anammox after inflow events in the central Baltic Sea, Limnology and Oceanography, 52, 1336-1345, 2007.
Hansen, H. P. and Koroleff, F.: Determination of nutrients. In: Methods of Seawater Analysis., Grasshoff, K., Kremling, K., and Ehrhardt, M. (Eds.), Willey-VCH, Weinheim, Germany, 1999.

Hansen, H. P. and Koroleff, F.: Determination of nutrients. In: Methods of Seawater Analysis, Wiley-VCH Verlag GmbH, 2007.
Hietanen, S., Jäntti, H., Buizert, C., Jürgens, K., Labrenz, M., Voss, M., and Kuparinen, J.: Hypoxia and nitrogen processing in the Baltic Sea water column, Limnology and Oceanography, 57, 325-337, 2012.
Holtermann, P. L., Prien, R., Naumann, M., Mohrholz, V., and Umlauf, L.: Deepwater dynamics and mixing processes during a major inflow event in the central Baltic Sea, Journal of Geophysical Research: Oceans, 122, 6648-6667, 2017.
Keil, R. G., Neibauer, J. A., Biladeau, C., van der Elst, K., and Devol, A. H.: A multiproxy approach to understanding the "enhanced" flux of organic matter through the oxygen-deficient waters of the Arabian Sea, Biogeosciences, 13, 2077-2092, 2016.
Knauer, G. A., Martin, J. H., and Bruland, K. W.: Fluxes of particulate carbon, nitrogen, and phosphorus in the upper water column of the northeast Pacific, Deep Sea Research Part A. Oceanographic Research Papers, 26, 97-108, 1979.
Kreus, M. and Schartau, M.: Variations in the elemental ratio of organic matter in the central Baltic Sea: Part II – Sensitivities of annual mass flux estimates to model parameter variations, Continental Shelf Research, 100, 46-63, 2015.
Kreus, M., Schartau, M., Engel, A., Nausch, M., and Voss, M.: Variations in the elemental ratio of organic matter in the central Baltic Sea: Part I—Linking primary production to remineralization, Continental Shelf Research, 100, 25-45, 2015.
Kullenberg, G. and Jacobsen, T. S.: The Baltic Sea: an outline of its physical oceanography, Marine Pollution Bulletin, 12, 183-186, 1981.
Le Moigne, F. A. C., Cisternas-Novoa, C., Piontek, J., Maßmig, M., and Engel, A.: On the effect of low oxygen concentrations on bacterial degradation of sinking particles, Scientific Reports, 7, 16722, 2017.
Legendre, L. and Gosselin, M.: New production and export of organic matter to the deep ocean: Consequences of some recent discoveries, Limnology and Oceanography, 34, 1374-1380, 1989.
Leipe, T., Tauber, F., Vallius, H., Virtasalo, J., Uścinowicz, S., Kowalski, N., Hille, S., Lindgren, S., and Myllyvirta, T.: Particulate organic carbon (POC) in surface sediments of the Baltic Sea, Geo-Marine Letters, 31, 175-188, 2011.
Lenz, C., Jilbert, T., Conley, D. J., Wolthers, M., and Slomp, C. P.: Are recent changes in sediment manganese sequestration in the euxinic basins of the Baltic Sea linked to the expansion of hypoxia?, Biogeosciences, 12, 4875-4894, 2015.
Lindroth, P. and Mopper, K.: High performance liquid chromatographic determination of subpicomole amounts of amino acids by precolumn fluorescence derivatization with o-phthaldialdehyde, Analytical Chemistry, 51, 1667-1674, 1979.
Logan, B. E., Passow, U., Alldredge, A. L., Grossartt, H.-P., and Simont, M.: Rapid formation and sedimentation of large aggregates is predictable from coagulation rates (half-lives) of transparent exopolymer particles (TEP), Deep Sea Research Part II: Topical Studies in Oceanography, 42, 203-214, 1995.
Long, R. A. and Azam, F.: Abundant protein-containing particles in the sea, Aquatic Microbial Ecology, 10, 213-221, 1996.
Mari, X. and Burd, A.: Seasonal size spectra of transparent exopolymeric particles (TEP) in a coastal sea and comparison with those predicted using coagulation theory, Marine Ecology Progress Series, 163, 13, 1998.
Mari, X., Passow, U., Migon, C., Burd, A. B., and Legendre, L.: Transparent exopolymer particles: Effects on carbon cycling in the ocean, Progress in Oceanography, 151, 13-37, 2017.
Mari, X., Rassoulzadegan, F., Brussaard, C. P. D., and Wassmann, P.: Dynamics of transparent exopolymeric particles (TEP) production by Phaeocystis globosa under N- or P-limitation: a controlling factor of the retention/export balance, Harmful Algae, 4, 895-914, 2005.

McDonnell, A. M. P., Boyd, P. W., and Buesseler, K. O.: Effects of sinking velocities and microbial respiration rates on the attenuation of particulate carbon fluxes through the mesopelagic zone, Global Biogeochemical Cycles, 29, 175-193, 2015.
Nausch, M., Nausch, G., Lass, H. U., Mohrholz, V., Nagel, K., Siegel, H., and Wasmund, N.: Phosphorus input by upwelling in the eastern Gotland Basin (Baltic Sea) in summer and its effects on filamentous cyanobacteria, Estuarine, Coastal and Shelf Science, 83, 434-442, 2009.
Neretin, L. N., Pohl, C., Jost, G., Leipe, T., and Pollehne, F.: Manganese cycling in the Gotland Deep, Baltic Sea, Marine Chemistry, 82, 125-143, 2003.
Passow, U.: Production of transparent exopolymer particles (TEP) by phyto- and bacterioplankton, Marine Ecology Progress Series, 236, 12, 2002.
Passow, U. and Alldredge, A. L.: A dye-binding assay for the spectrophotometric measurement of transparent exopolymer particles (TEP), Limnology and Oceanography, 40, 1326-1335, 1995.
Pohl, C., Löffler, A., and Hennings, U.: A sediment trap flux study for trace metals under seasonal aspects in the stratified Baltic Sea (Gotland Basin; 57°19.20'N; 20°03.00'E), Marine Chemistry, 84, 143-160, 2004.
Redfield, A. C., Ketchum, B. H., and Richards, F. A.: The Influence of Organisms on the Composition of the Sea Water. In: The Sea, Hill, M. N. (Ed.), Interscience Publishers, New York, 1963.
Richardson, L. L., Aguilar, C., and Nealson, K. H.: Manganese oxidation in pH and O2 microenvironments produced by phytoplankton1,2, Limnology and Oceanography, 33, 352-363, 1988.
Sandberg, J., Elmgren, R., and Wulff, F.: Carbon flows in Baltic Sea food webs — a re-evaluation using a mass balance approach, Journal of Marine Systems, 25, 249-260, 2000.
Schmale, O., Krause, S., Holtermann, P., Power Guerra, N. C., and Umlauf, L.: Dense bottom gravity currents and their impact on pelagic methanotrophy at oxic/anoxic transition zones, Geophysical Research Letters, 43, 5225-5232, 2016.
Shaffer, G.: Phosphate pumps and shuttles in the Black Sea, Nature, 321, 515, 1986.
Stigebrandt, A.: Computations of oxygen fluxes through the sea surface and the net production of organic matter with application to the Baltic and adjacent seas, Limnology and Oceanography, 36, 444-454, 1991.
Strickland, J. D. and Parsons, T. R.: Determination of dissolved oxygen. In: A Practical Handbook of Seawater Analysis, Fisheries Research Board of Canada, 1968.
Strickland, J. D. H., Parsons, T. R., and Strickland, J. D. H.: A practical handbook of seawater analysis, Fisheries Research Board of Canada, Ottawa, 1972.
Thomas, H. and Schneider, B.: The seasonal cycle of carbon dioxide in Baltic Sea surface waters, Journal of Marine Systems, 22, 53-67, 1999.
Trull, T. W., Bray, S. G., Buesseler, K. O., Lamborg, C. H., Manganini, S., Moy, C., and Valdes, J.: In situ measurement of mesopelagic particle sinking rates and the control of carbon transfer to the ocean interior during the Vertical Flux in the Global Ocean (VERTIGO) voyages in the North Pacific, Deep Sea Research Part II: Topical Studies in Oceanography, 55, 1684-1695, 2008.
Turner, J. T.: Zooplankton fecal pellets, marine snow, phytodetritus and the ocean's biological pump, Progress in Oceanography, 130, 205-248, 2015.
van Mooy, B. A. S., Keil, R. G., and Devol, A. H.: Impact of suboxia on sinking particulate organic carbon: Enhanced carbon flux and preferential degradation of amino acids via denitrification, Geochimica et Cosmochimica Acta, 66, 457-465, 2002.
Wasmund, N.: Occurrence of cyanobacterial blooms in the baltic sea in relation to environmental conditions, Internationale Revue der gesamten Hydrobiologie und Hydrographie, 82, 169-184, 1997.
Wasmund, N. and Uhlig, S.: Phytoplankton trends in the Baltic Sea, ICES Journal of Marine Science, 60, 2003.
Wilhelm, W. L.: Die Bestimmung des im Wasser gelösten Sauerstoffes, Berichte der deutschen chemischen Gesellschaft, 21, 2843-2854, 1888.

Biogeosciences Discuss., https://doi.org/10.5194/bg-2018-360
Manuscript under review for journal Biogeosciences
Discussion started: 6 August 2018

Figure Captions

Figure 1. Monthly averaged Chl *a* distribution derived from VIIRS for June 2015 in the Baltic Sea. Black circle and "x" indicate the position of the trap deployment and the seawater collection respectively in Gotland Deep (GB) and Landsort Deep (LD). The lower panel shows the trajectory of the trap deployed at GB and LD.

Figure 2. Water column profiles at the location of the sediment trap deployments in (A) the GB, and (B) the LD. Left panel: oxygen (blue), temperature (red), and salinity (black). Middle panel: nitrate (NO_3), nitrite (NO_2), and ammonium (NH_4). Right panel: phosphate (PO_4), and silicate ($Si(OH)_4$). Grey lines indicate the depths at which we deployed sediment traps.

Figure 3. Particulate organic matter profiles in the water column at the location of the sediment traps deployments in the GB (A, B and C) and the LD (D, E and F). (A and D) particulate organic carbon (POC), particulate nitrogen (PN), and particulate organic phosphorous (POP). (B and E) chlorophyll a (Chl a) and biogenic silicate (BSi). (C and F) transparent exopolymeric particles (TEP) and Coomassie stainable particles (CSP). Grey lines as figure 2.

Figure 4. MnOx-like containing particles and O_2 concentration profiles in the water column at the location of the sediment traps deployments. (A) the GB and (B) the LD. Grey lines as in figure 3.

Figure 5. Particulate organic matter fluxes in the GB (A and B) and the LD (C and D) . (A and C) POC, PN and O_2. (B and D) POP, Chl a, and BSi.

Figure 6. TEP and CSP fluxes in the GB (A and B) and the LD (C and D). In addition to the vertical distribution of the flux, each profile is complemented with images captured under the microscope (200x) at each depth. Star-shaped MnOx-like particles are clearly visible in the GB associated to TEP (A), but not with CSP (B). MnOx-like particles were significantly less abundant in the LD (C and D). (F) A larger magnification (400x) image of MnOx-like particles at 110 m showing more detail on the shape of those particles and aggregates formed with TEP.

Biogeosciences Discuss., https://doi.org/10.5194/bg-2018-360
Manuscript under review for journal Biogeosciences
Discussion started: 6 August 2018

Figure 7. Total hydrolyzable amino acids (TAA) and total carohydrates (TCHO) fluxes in (A) the GB, and (B) the LD.

Biogeosciences Discuss., https://doi.org/10.5194/bg-2018-360
Manuscript under review for journal Biogeosciences
Discussion started: 6 August 2018

Table 1. Sediment traps deployment and recovery locations, dates, collection times and depths.

Station	Lat	Lon	Date	Station depth	Deployment time (d)	Trap depths (m)
Gotland Basin (GB)	57.21 °N	20.03 °E	08/06/2015	248 m	2	40A, 40B, 60, 110, and 180m
	57.27 °N	20.25 °E	10/06/2015			
Landsort Deep (LD)	58.69 °N	18.55 °E	15/06/2015	460 m	1	40A, 40B, 55, 110, and 180m
	58.68 °N	18.68 °E	16/06/2015			

Biogeosciences Discuss., https://doi.org/10.5194/bg-2018-360
Manuscript under review for journal Biogeosciences
Discussion started: 6 August 2018

Table 2. Abundance of chlorophyll and phycoerythrin containing pico- and nanoplankton measured by flow-cytometry in the GB and the LD.

		Phytoplankton (mL^{-1})			Cyanobacteria-like cells (mL^{-1})		
	Depth (m)	picoplankton	nanoplankton	Total	picoplankton	nanoplankton	Total
GB	1	87963	2097	90060	5225	731	5956
	10	94369	2628	96997	8795	920	9716
	40	4999	68	5067	2174	69	2243
	60	4125	35	4160	1990	42	2032
	80	599	7	606	238	15	253
	110	594	7	601	326	29	356
	140	1144	14	1158	356	2	358
	180	908	9	917	366	20	385
	220	2270	19	2289	1063	34	1097
LD	1	92359	2283	94642	834	177	1011
	10	86426	1708	88134	2990	232	3223
	40	2022	92	2114	2243	69	2312
	60	1524	62	1586	1294	24	1318
	70	908	43	951	613	17	630
	110	1735	82	1817	1181	17	1198
	180	1339	75	1415	946	34	980
	250	1593	82	1676	949	36	985
	300	1521	48	1569	1047	17	1064
	350	1608	57	1665	908	12	920
	400	1548	73	1621	1047	22	1069
	430	1562	68	1631	875	19	894

Biogeosciences Discuss., https://doi.org/10.5194/bg-2018-360
Manuscript under review for journal Biogeosciences
Discussion started: 6 August 2018

Table 3. Phytoplankton abundances analyzed microscopically in the GB and the LD, volume analyzed was 50 ml per sample.

		GB (cells mL^{-1})				LD (cells mL-1)			
		1 m	10 m	40 m	Total	1 m	10 m	40 m	Total
Cyanophyceae *	Total	14148	13536	0	27684	37368	32526	96	69990
Chryptophyta	Total	140	112	28	280	1400	882	56	2338
Bacillariophyceae	Total	96	94	44	234	462	112	102	676
	Chaetoceros sp.	58	42	24	124	434	106	26	566
	Skeletonema sp.	26	8	12	46	12	0	8	20
	Thalassiosira sp.	12	44	8	64	16	6	68	90
Dinophyceae	Total	3772	4424	1192	9388	9032	7662	1404	18098
	Dinophysis sp.	678	742	2	1422	450	214	4	668
	other	3094	3682	1190	7966	8582	7448	1400	17430
Chlorophyta	Total	5320	6860	28	12208	2072	1022	238	3332
	Planctonema sp.	5320	6860	28	12208	2072	1022	238	3332

* >90% were filamentous unicellular cyanobacteria *Aphanizomenon* sp.

Biogeosciences Discuss., https://doi.org/10.5194/bg-2018-360
Manuscript under review for journal Biogeosciences
Discussion started: 6 August 2018

Table 4. MnOx-like particles fluxes and size determined by image analysis in GB and LD.

Station	Depth (m)	MnOx-like particles (cm^2 $m^{-2}d^{-1}$)	Median size ESD (μm)	Size range ESD (μm)
GB	110	5666.1± 993.5	2.8	0.6-166.7
	180	7789.1± 954.7	3.3	0.6-152.7
LD	110	50.3±1.8	1.8	0.6-16.5
	180	2.6±0.3	1.4	1.2-9.3

Biogeosciences Discuss., https://doi.org/10.5194/bg-2018-360
Manuscript under review for journal Biogeosciences
Discussion started: 6 August 2018

Table 5. Amino acids (AA), carbohydrates (CHO) and elemental molar ratios of sinking and suspended OM in the GB and in the LD.

	Depth (m)	AA-C:POC %	CHO-C:POC %	POC:PN	POC:POP	POC:Bsi	PN:POP
GB sinking OM	40	19.19	18.26	9.80	244.05	3.86	0.39
	40	17.58	17.21	9.43	222.42	4.07	0.43
	60	15.78	17.56	9.52	231.56	2.78	0.29
	110	13.87	22.24	11.31	90.12	1.73	0.15
	180	11.13	18.47	12.68	122.87	2.97	0.23
LD sinking OM	40	13.52	9.43	12.17	771.70	3.58	0.29
	40	14.27	8.40	11.09	413.14	4.12	0.37
	55	19.10	10.97	12.43	331.81	3.03	0.24
	110	13.37	11.97	15.44	229.70	2.67	0.17
	180	14.32	12.85	15.29	341.33	4.19	0.27
GB suspended OM	1	8.22	16.94	10.39	154.56	91.45	14.88
	10	10.81	8.84	10.48	150.51	87.15	14.36
	40	4.91	2.80	9.19	88.78	133.75	9.66
	60	5.43	2.66	9.78	127.36	125.24	13.02
	80	4.67		10.43	144.92		13.89
	110	9.01	6.63	8.45	245.26		29.01
	140	5.34		10.60	283.42		26.73
	180	5.73	4.29	11.37	506.21		44.54
	220	8.57	3.35	12.06	270.78		22.45
LD suspended OM	1	6.96		8.66	205.29	514.94	23.71
	10	12.97	9.12	8.43	196.44	100.91	23.31
	40	0.00	8.88	8.09	335.66	24.48	41.51
	60	6.09	10.26	7.83	300.75	16.89	38.43
	70	7.92	10.72	7.71	291.81	247.80	37.86
	110	12.22	5.41	7.93	224.56		28.32
	180	10.12	11.32	7.02	205.33		29.23
	250	11.97	8.81	6.52	249.36		38.22
	300	10.88		6.71	136.67		20.37
	350	10.67	10.12	6.76	145.80		21.56
	400	9.99		6.18	229.53		37.16
	430	9.35	9.45	7.82	148.61		19.01

Biogeosciences Discuss., https://doi.org/10.5194/bg-2018-360
Manuscript under review for journal Biogeosciences
Discussion started: 6 August 2018

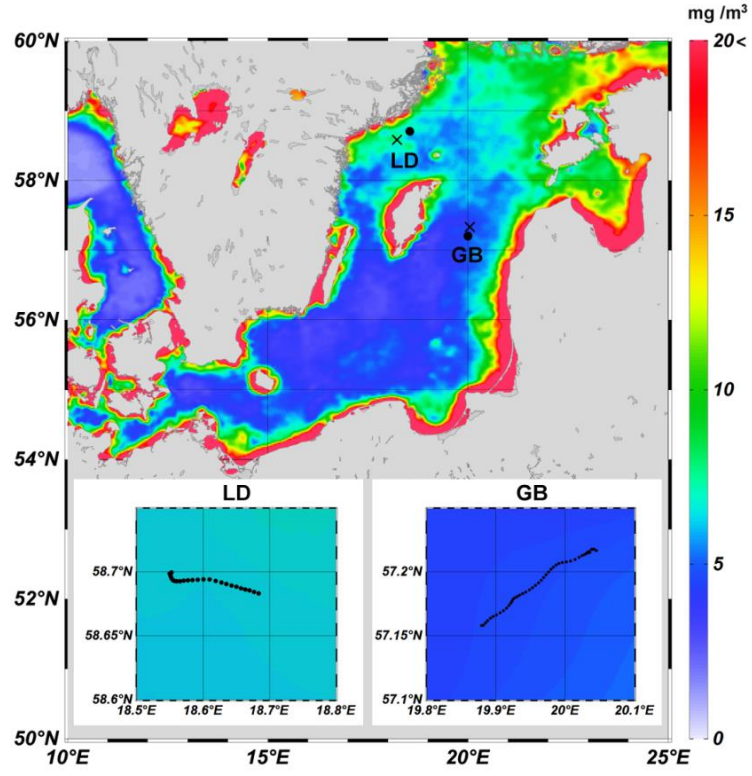

Fig. 1

Biogeosciences Discuss., https://doi.org/10.5194/bg-2018-360
Manuscript under review for journal Biogeosciences
Discussion started: 6 August 2018

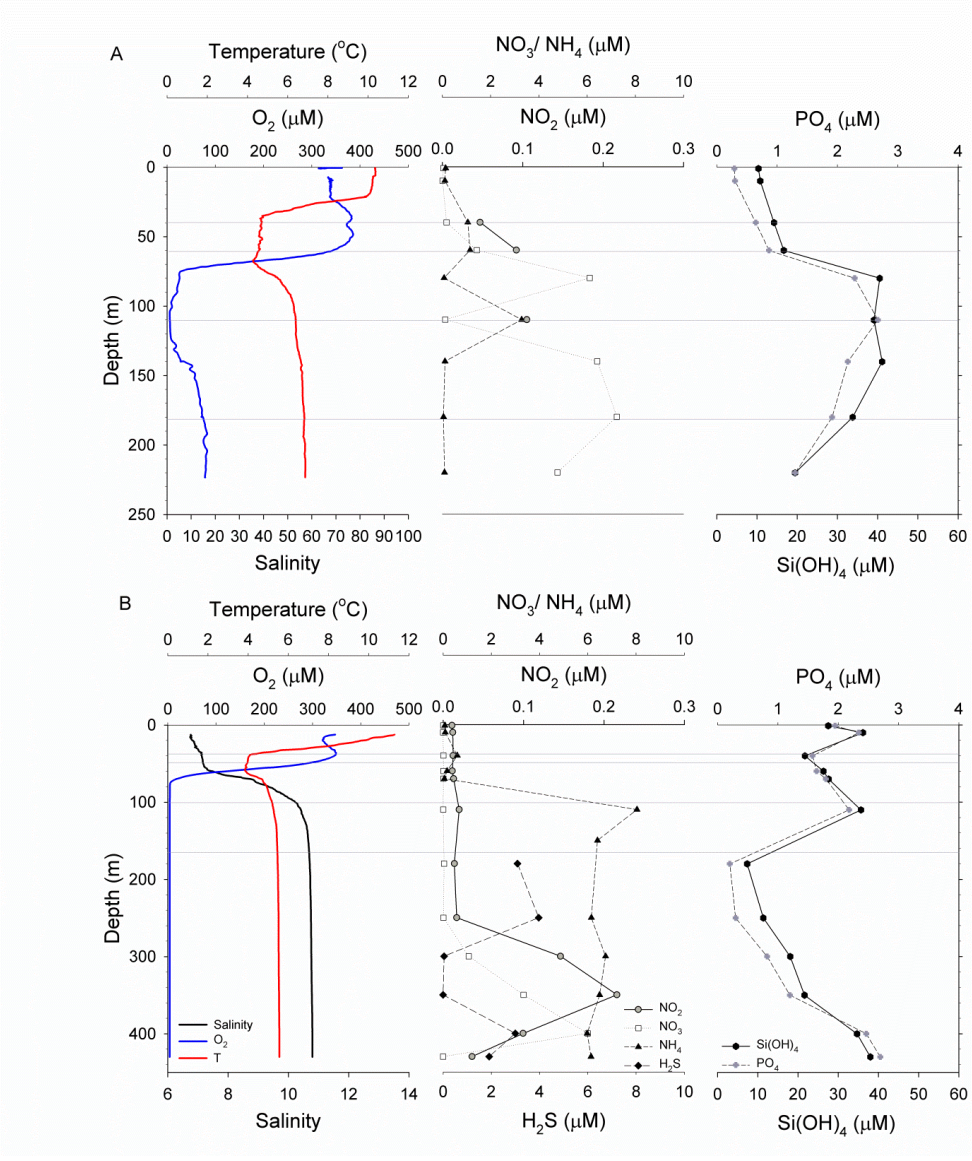

Fig. 2

Biogeosciences Discuss., https://doi.org/10.5194/bg-2018-360
Manuscript under review for journal Biogeosciences
Discussion started: 6 August 2018

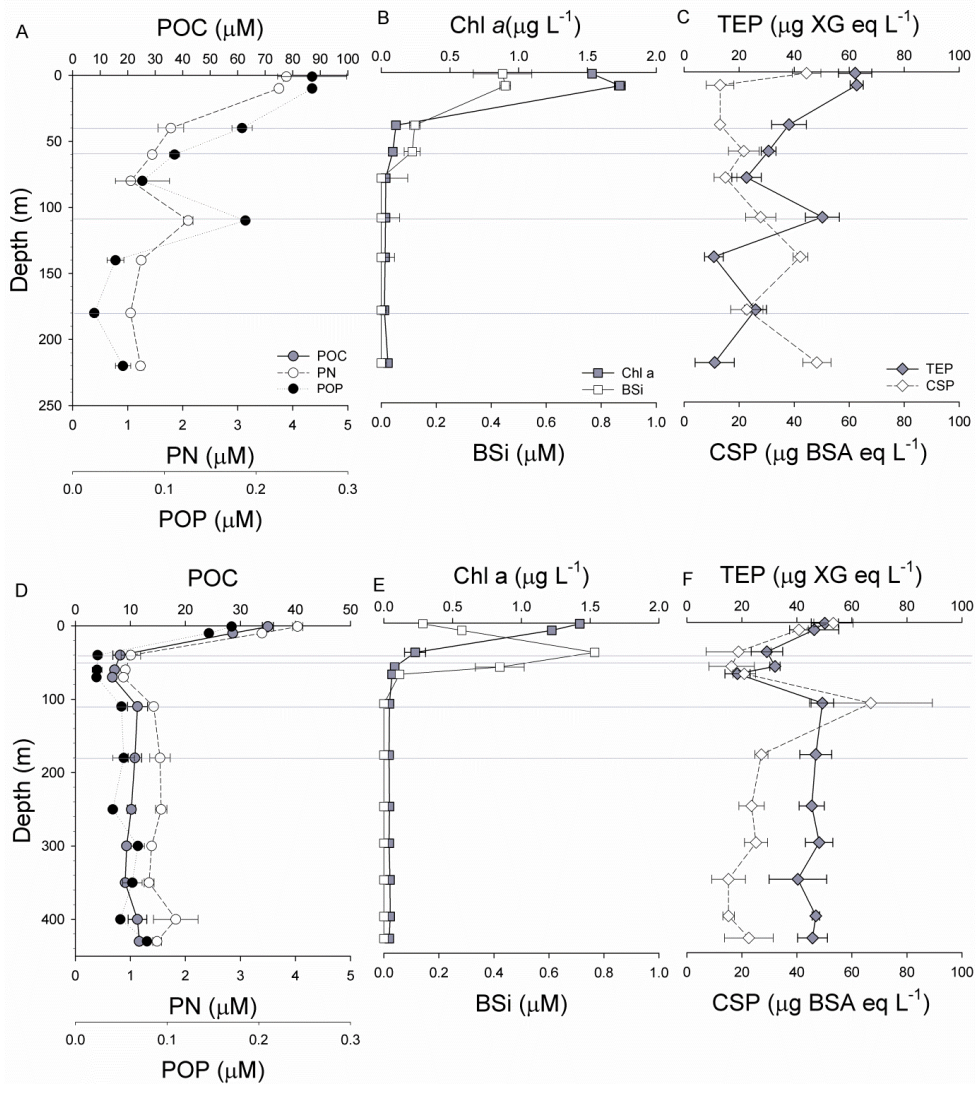

Fig. 3

Biogeosciences Discuss., https://doi.org/10.5194/bg-2018-360
Manuscript under review for journal Biogeosciences
Discussion started: 6 August 2018

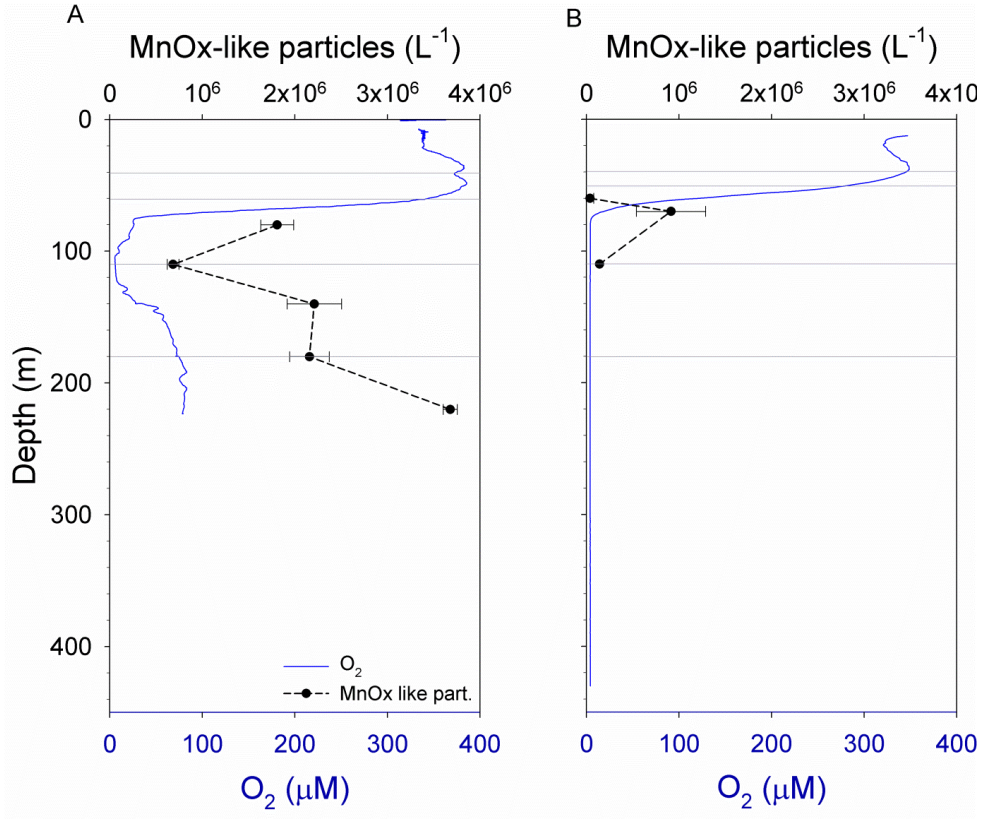

Fig. 4

Biogeosciences Discuss., https://doi.org/10.5194/bg-2018-360
Manuscript under review for journal Biogeosciences
Discussion started: 6 August 2018

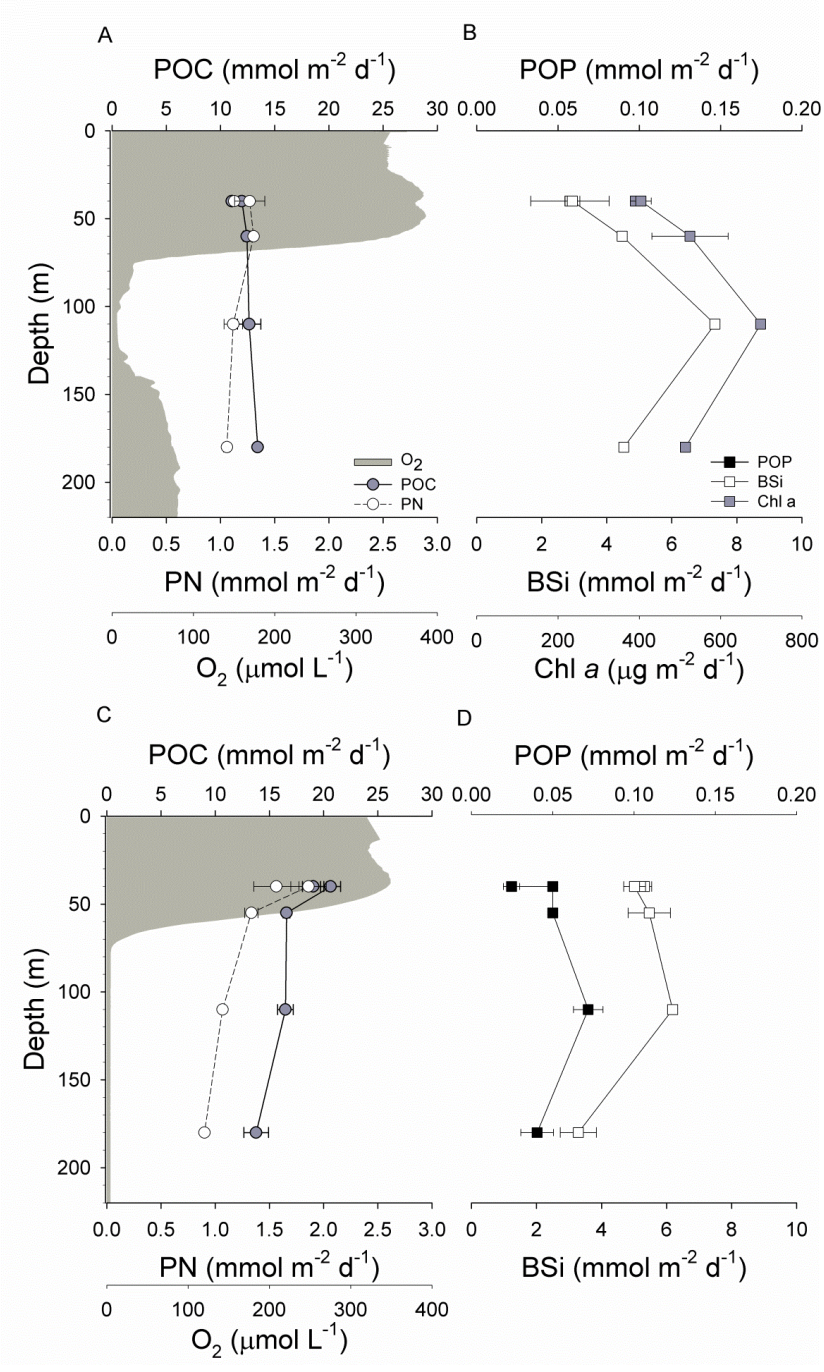

Fig. 5

Biogeosciences Discuss., https://doi.org/10.5194/bg-2018-360
Manuscript under review for journal Biogeosciences
Discussion started: 6 August 2018

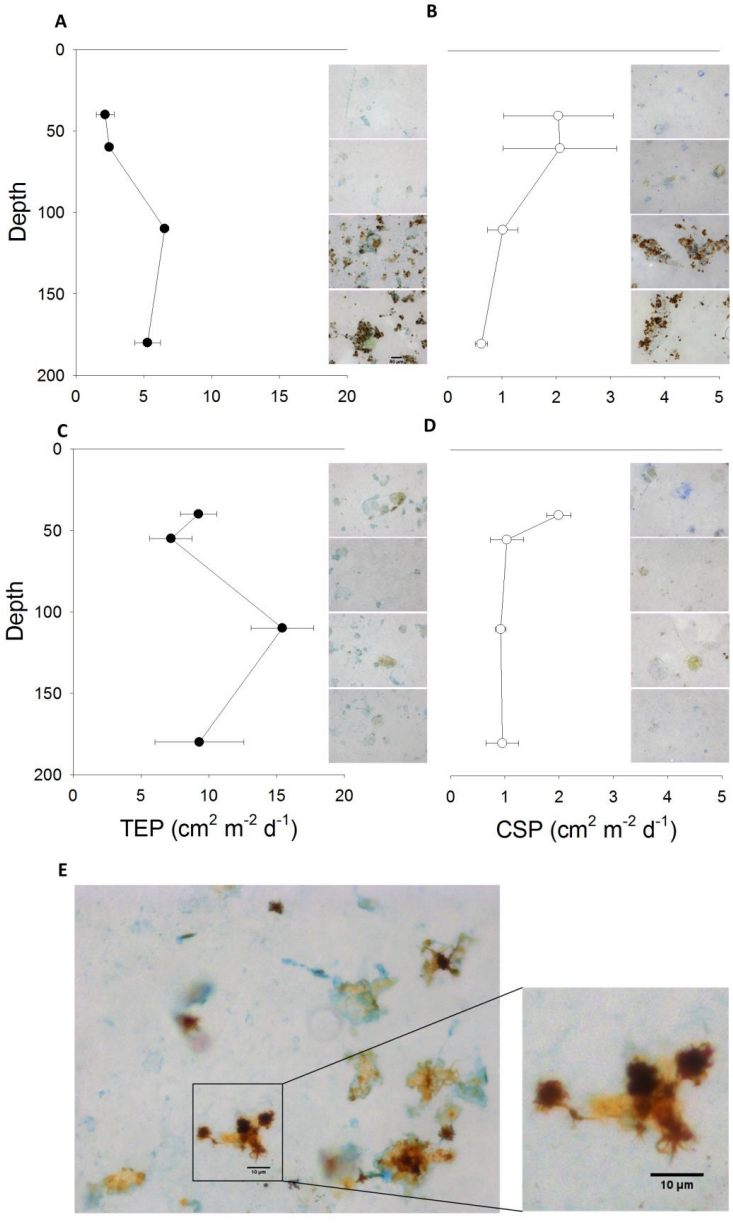

Fig. 6

Biogeosciences Discuss., https://doi.org/10.5194/bg-2018-360
Manuscript under review for journal Biogeosciences
Discussion started: 6 August 2018

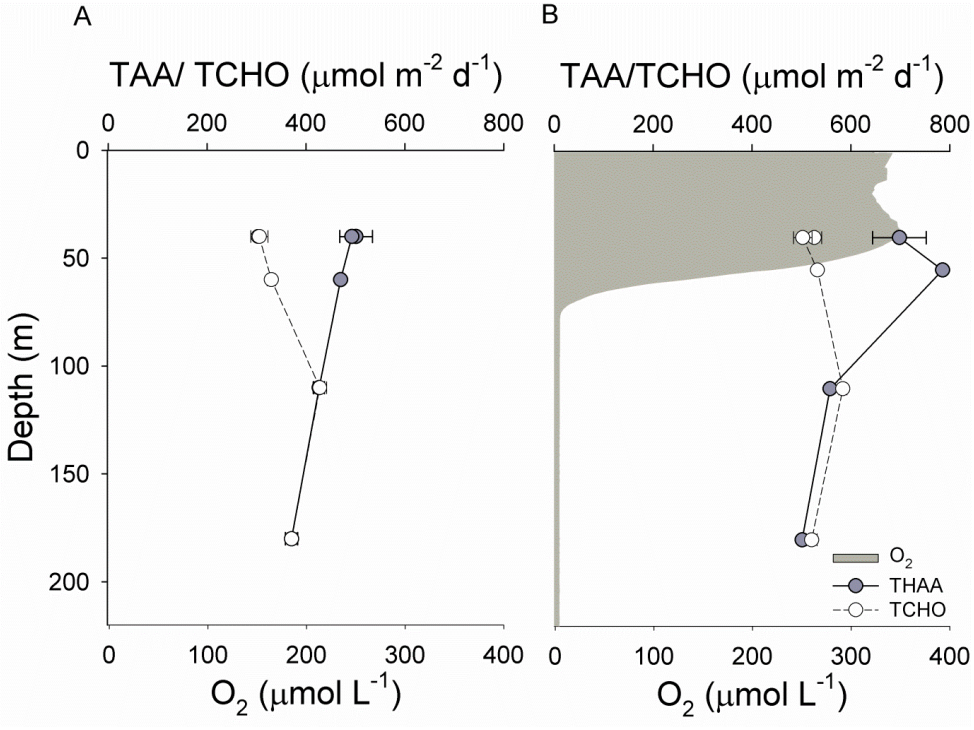

Fig. 7